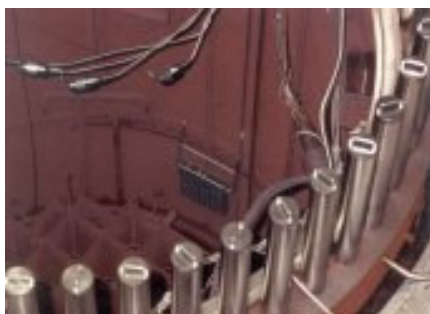


Deposition of CRUD in BWR water on various steels exposed in the Dodewaard nuclear power plant

W.M.M. Huijbregts¹ & P.J.C. Letschert²

Kema Scientific & Technical Reports 4 (2): 15-25. ISSN 0167-8590; ISBN 90-353-0037-8. (paper 33)

JAF conference Tokio 1987



Rack with samples exposed in the reactor vessel of the GKN boiling-water reactor in Dodewaard

Abstract

A rack composed of different materials and surface treatments was exposed in the reactor vessel of the GKN boiling-water reactor in Dodewaard for one reactor cycle in order to study the CRUD (Corrosion Residual Unidentified Deposit) deposition. Ferritic, austenitic and ferritic-austenitic steels and Inconel 600 were mounted in the rack. The Co-60 and Mn-54 activity of the CRUD and of the adherent oxide layer were measured.

The more CRUD was deposited on the samples, the higher the Co-60 and Mn-54 activities of the adherent oxide layer appeared to be. The Co-60 activity of the adherent oxide layer increased greatly with higher CRUD deposition for the high-chromium austenitic steels. The effect of CRUD deposition on Co-60 activity of the adherent oxide layer was slight for the ferritic low-chromium steels and for Inconel 600. The influence of CRUD deposition on the Mn-54 activity of the adherent oxide layer was greater for the ferritic steels than it was for the austenitic steels. The surface pretreatments of AISI 304, annealing in air at 623 K and autoclaving at 583 K, resulted in higher activity levels.

Introduction

The Dodewaard nuclear power plant has been in service since 1969 and is a boiling-water reactor (BWR) with natural circulation of an adapted General Electric design from the early sixties. It is a pilot plant of, nowadays, 60 MWe (183 MWth). During the research program described here, the reactor had not yet been upgraded and had a rated power of 54 MWe (163.4 MWth). The scheme of the power plant is given in Figure 1.

¹ N.V.KEMA R&D Division, Department of Chemical Research, P.O.Box 9035, 6800 ET, ARNHEM, The Netherlands.

² N.V.GKN, Waalbandijk 112a, 669 MG, DODEWAARD, The Netherlands

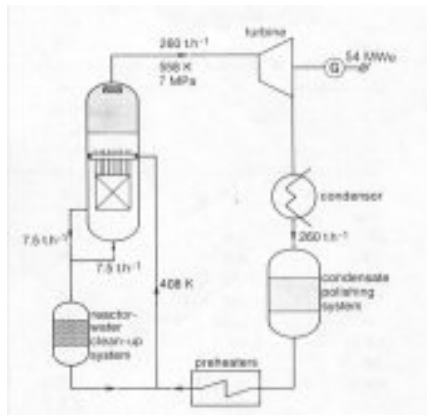


Figure 1 Flow scheme of the Dodewaard BWR in 1981

The reactor vessel contains 164 fuel elements which produce a steam flow of 260 t.h.⁻¹. Pressure and temperature during the investigations described here were 7 MPa and 558 K respectively. After the upgrading from 54 to 60 MWe in 1984 the values are 7.6 MPa and 564 K respectively.

The steam passes the turbine, condenser, a 100% mixed bed filter demineralizer, stainless steel preheaters and returns to the reactor vessel. The reactor water clean-up system (RWCU) consists of a mixed bed filter demineralizer. The capacity is 15 t./h, being 6% of the feedwater flow.

The radiation levels are generally rather low. Nevertheless the pipe from the reactor vessel to the reactor-water clean-up system has a high exposure rate because of CRUD (Corrosion Residual Unidentified Deposit) deposition. Samples were taken from this pipe for microscopic examination in 1980.

The oxide consisted of two layers, a loose outer layer (mainly Fe₂O₃) and an adherent layer of Fe-Cr-Ni oxides. Ultrasonic cleaning of the samples removed the hematite but did not greatly decrease the activity. Exposure rates of 0.7 R./h and 0.5 R/h were measured on the surface of the sample before and after ultrasonic cleaning respectively. Pickling of the samples removed the adherent oxide and lowered the activity to below the detection limit.

Deposition of CRUD and incorporation of Co-60 in the adherent oxide layers were considered to be influenced by the solubility of the CRUD, which is controlled by factors such as pH, O₂ content, ECP (Electrochemical Corrosion Potential), conductivity and temperature. Time was lacking to carry out an extensive research program on the problem of CRUD deposition. A sample rack was therefore constructed, which was composed of different steels with various types of surface pretreatments. It was exposed in the reactor vessel of the Dodewaard BWR for one reactor cycle.

Table 1 Average value of the water quality, April 1981 to February 1982

| | | Reactor water at GKN | Specification 1980 | | Feedwater at GKN | Steam at GKN |
|------------------|------------------|----------------------------|--------------------|------|---------------------|-----------------|
| | | | GE | VGB | | |
| spec. cond. | $\mu\text{S/m}$ | 8 | 100 | 100 | 4.5 | 7.8 |
| SiO ₂ | $\mu\text{g/l}$ | 119 | | 4000 | | 1 |
| O ₂ | $\mu\text{g/l}$ | 123 | 200 | | 24 | |
| Fe | $\mu\text{g/l}$ | 20 | 25 | | 6 | |
| Cu | $\mu\text{g/l}$ | 2 | 7 | | <1 | |
| C1 | $\mu\text{g/l}$ | < 50 | 200 | 200 | | |
| total y-act. | $\mu\text{Ci/l}$ | 27.4 | | | 0.03 | 2,6 |
| Cr-51 | $\mu\text{Ci/l}$ | 2,2 | | | | |
| Mn-54 | $\mu\text{Ci/l}$ | 0.6 | | | | |
| Fe-59 | $\mu\text{Ci/l}$ | 0.3 | | | | |
| Co-58 | $\mu\text{Ci/l}$ | 0.2 | | | | |
| Co-60 | $\mu\text{Ci/l}$ | 0.7 | | | | |

Exposure conditions

During the exposure time of 6500 h from April 1981 to January 1982, the sample rack was located in the reactor vessel above the feedwater inlet sparger (Fig. 2). The reactor was operated at full power during this period, without any shutdown.

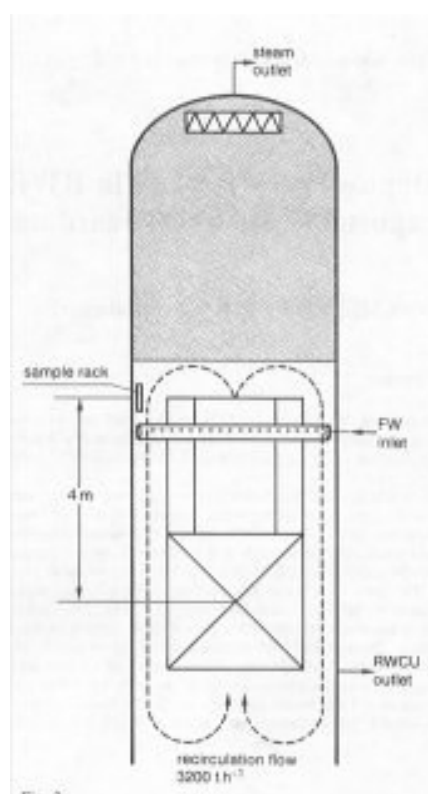


Figure 2. Position of the sample rack in the reactor vessel

The reactor water is circulated internally in the reactor vessel by natural circulation with a flow of about 3200 t/h. There is a two-phase flow at the site of the sample rack; the void is about 50% at full power. Table 1 provides the data on the quality of the reactor water, feedwater and steam. The figures were averaged for exposure time. As can be seen, the values are far below the general specifications for the quality of the reactor water.

Figures 3 and 4 show the rack with the samples before exposure. The tube length of the samples was 40 mm and their diameter ranged from 18.8 to 45 mm. The diameter and the chemical analysis of the samples are given in Table 2. The samples consisted of four ferritic, six austenitic and one ferritic-austenitic steel specimen. All samples had been glass-blasted as a surface pretreatment.

Table 2 Chemical analysis of the samples.

| material | diameter (mm) | weight percentage | | | | | | | | | | | structure |
|-------------|------------------|----------------------|------|------|-------|-------|------|------|------|------|------|-------|----------------------|
| | | C | Mn | Si | P | S | Cr | Ni | Cu | Mo | Co | Ti | |
| C-steel | 45.0 | 0.51 | 0.51 | 0.14 | 0.008 | 0.016 | 0.03 | 0.02 | 0.04 | 0.01 | - | - | ferritic |
| 15Mo3 | 44.6 | 0.16 | 0.70 | 0.19 | 0.006 | 0.019 | 0.02 | 0.02 | 0.04 | 0.28 | - | - | ferritic |
| 14Mn4 | 38.0 | 0.12 | 0.98 | 0.37 | 0.012 | 0.010 | 0.04 | 0.03 | 0.03 | 0.02 | - | - | ferritic |
| 10CrMo910 | 44.4 | 0.06 | 0.52 | 0.18 | 0.017 | 0.032 | 2.51 | 0.12 | 0.16 | 0.93 | - | - | ferritic |
| AISI304 | 25.1 | 0.020 | 0.12 | 0.49 | 0.026 | 0.012 | 18.6 | 10.2 | 0.17 | 0.20 | -- | -- | austenitic |
| AISI316 | 18.8 | 0.046 | 1.77 | 0.59 | 0.018 | 0.012 | 17.1 | 13.0 | 0.12 | 2.76 | -- | <0.02 | austenitic |
| 254SM0 | 25.4 | 0.020 | 0.54 | 0.44 | 0.021 | 0.015 | 19.5 | 17.5 | 0.85 | 6.30 | -- | -- | austenitic |
| A16X | 25.4 | 0.016 | 1.47 | 0.38 | 0.019 | 0.001 | 20.4 | 24.2 | 0.10 | 6.50 | -- | -- | austenitic |
| Incoloy 800 | 22.0 | 0.023 | 0.50 | -- | -- | 0.002 | 20.8 | 34.0 | 0.01 | -- | 0.08 | 0.38 | austenitic |
| Incone1600 | 21.3 | 0.050 | 0.14 | 0.36 | 0.006 | 0.006 | 15.9 | 74.4 | 0.08 | 0.08 | 0.20 | 0.35 | austenitic ferr.- |
| Uranus 50 | 18.8 | 0.025 | 1.42 | 0.56 | 0.026 | 0.008 | 21.6 | 6.5 | 1.56 | 2.62 | 0.11 | -- | aust.. |



Figure 3 Samples mounted in the rack, before exposure. Flow direction from left to right.

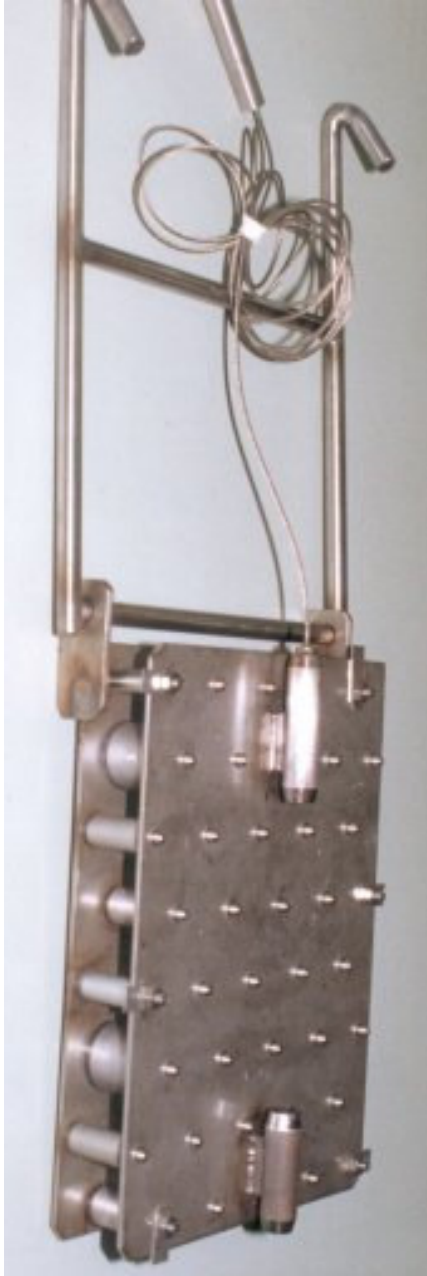


Figure 4. The sample rack, ready for exposure in the reactor vessel.

The influence of some special surface pretreatments was one of the aspects to be investigated. The AISI 304 and AISI 316 samples were therefore pre-treated by glass blasting, pickling, passivating, steam autoclaving and air annealing. Details of the surface pretreatments are given in Table 3.

Table 3 Surface pre-treatment for AISI 304 and AISI 316 samples.

- 1 glass blasting
- 2 glass blasting and pickling in 15% HNO_3 + 5% $\text{NH}_4 \text{HF}_2$ at 333 K
- 3 glass blasting and pickling and passivating in 20% HNO_3 at 298 K
- 4 glass blasting and autoclaving in steam at 583 K for 24 h
- 5 glass blasting and annealing in air at 623 K for 8 h

The samples were mounted in the rack by means of pre-oxidized zircaloy insulator rings to prevent electrochemical influences. Following exposure, the sample rack was removed from the reactor vessel and stored in the spent-fuel pool for decay of the short- living isotopes. After half a year of storage, the exposure rate of the entire rack was still 5 R.h^{-1} with a shielding of 0.5 m water.

The sample rack was opened under water with handling tools and the samples were removed very carefully and stored in plastic bottles. Only very small amounts of CRUD were lost during this handling.

The exposure rate on the sample surfaces varied between 10^{-2} and 10^{-1} R.h^{-1} .

Results

The activity levels and the morphology of the samples after CRUD deposition were the object of special attention during the work reported here.

Activity

The activity of the samples with the CRUD was measured with a 10% high-purity Ge-detector and a 4000-channel multichannel analyzer (detector Canberra model 7229P, analyzer Canberra S40). The distance of the samples from the detector was 75 cm. Co-60 and Mn-54 activity was calculated from the gamma spectra per unit area of sample surface. The statistical counting error (3 σ) was < 1%. After measurement of the activity, the samples were cleaned ultrasonically in water with a wetting agent added for 45 minutes (US cleaner Sonogen model L TH 80/4R, average power 150 W, peak power 300 W and 24.4 kHz). Subsequently the samples were flushed and measured again.

The results of the activity measurements are given in Tables 4 and 5. The values (for AISI 304 and 316 the average values) were plotted as bar diagrams (Figs. 5 and 6).

Table 4. Results of activity measurements and calculated CRUD deposition.

| material | position | activity Co-60/Mn-54 ($\mu\text{Ci}/\text{cm}^2$) | | amount of CRUD (mg/cm ²) filtered | calculated** | |
|-----------|----------|---|----------------|--|--------------|-------|
| | | CRUD + adherent oxide | adherent oxide | | Co-60 | Mn-54 |
| C-steel | C-5 | 4,14/3.00 | 1.85/0.49 | 1.9±0.01 | 0.63 | 0.92 |
| 15Mo3 | B-1 | 4.24/3.26 | 1.33/1.30 | | 0.80 | 1.08 |
| 14Mn4 | H-1 | 3.60/2.84 | 1.97/0.22 | | 0.45 | 0.96 |
| IOCrMo910 | G-5 | 6.96/3.03 | 2.17/0.23 | 12.5±0.01 | 1.32 | 1.02 |
| AISI304 | E-5 | 4.67/1.47 | 3.36/0.12 | 0.4±0.01 | 0.36 | 0.50 |
| | A-5 | 4.27/1.12 | 2.94/0.02 | | 0.37 | 0.40 |
| AISI316 | D-4 | 7.18/1.60 | 4.38/0.02 | 0.6±0.02 | 0.77 | 0.58 |
| | H-4 | 7.25/1.42 | 5.38/0.05 | | 0.51 | 0.50 |
| 254SM0 | E-4 | 7.72/1.79 | 5.31/0.09 | 0.7±0.01 | 0.66 | 0.62 |
| | E-2 | 7.84/1.76 | 5.63/0.08 | | 0.61 | 0.61 |
| A16X | D-1 | 6.13/1.36 | 4.60/0.02 | | 0.42 | 0.49 |
| | D-2 | 6.68/1.55 | 4.68/0.01 | | 0.55 | 0.56 |
| Inc. 800 | F-4 | 4.80/1.14 | 3.27/0.02 | 0.2±0.02 | 0.42 | 0.41 |
| | G-1* | 4.15/1.18 | 2.52/0.02 | | 0.46 | 0.42 |
| Inc.600 | F-5* | 8.74/2.99 | 3.37/0.45 | | 1.48 | 0.93 |
| | B-5* | 2.33/0.62 | 1.42/0.04 | | 0.25 | 0.21 |
| Ur50 | B-2 | 9.55/2.27 | 6.73/0.01 | 0.9±0.02 | 0.78 | 0.82 |
| | C_1* | 9.18/1.89 | 6.70/0.04 | | 0.68 | 0.68 |

*outside position

** calculated from specific activity

Co-60 = 3.64±0.70 $\mu\text{Ci}/\text{mg}$ Mn-54 = 2.74±0.44, $\mu\text{Ci}/\text{mg}$

Table 5 Results of activity measurements and calculated Crud deposition.

| material | position | activity Co-60/Mn-54 ($\mu\text{Ci}/\text{cm}^2$) | | | amount of CRUD mg/cm^2 | | |
|------------------------------|------------------------------|---|-------------------|-----------|--|-----------------------|------|
| | | CRUD + adherent oxide | adherent oxide | filtered | calculated** Co-60 | calculated** Mn-54 | |
| AISI 304 | glass | E-5 | 4.67/1.47 | 3.36/0.12 | 0.4±0.01 | 0.36 | 0.50 |
| | blasted | A-5 | 4.27/1.12 | 2.94/0.02 | | 0.37 | 0.40 |
| | glass | F-1 | 6.06/1.64 | 3.94/0.04 | | 0.58 | 0.58 |
| | blasted + pickled | D-3 | 5.99/1.60 | 3.82/0.01 | | 0.60 | 0.58 |
| | glass | B-3 | 6.63/2.04 | 3.90/0.02 | | 0.75 | 0.74 |
| | blasted+ pick. + pass. | A-4 | 6.19/1.82 | 3.87/0.03 | | 0.64 | 0.65 |
| | glass | F-2 | 9.14/1.86 | 5.92/0.09 | | 0.89 | 0.65 |
| | blasted+ autoclaved | E-1* | 5.91/1.26 | 4.33/0.05 | | 0.43 | 0.44 |
| | glass | F-3 | 9.24/2.31 | 5.80/0.12 | | 0.95 | 0.80 |
| | blasted+ annealed | C-3 | 9.44/2.33 | 5.41/0.09 | | 1.11 | 0.82 |
| | AISI 316 | glass | D-4 | 7.18/1.60 | 4.38/0.02 | 0.6±0.02 | 0.77 |
| blasted | | H-4 | 7.25/1.42 | 5.38/0.05 | | 0.51 | 0.50 |
| glass | | A-1* | 3.62/0.93 | 2.48/0.01 | | 0.32 | 0.34 |
| blasted + pickled | | A-2 | 7.48/1.87 | 4.96/0.02 | | 0.69 | 0.67 |
| glass | | B-4 | 6.48/1.53 | 4.41/0.02 | | 0.57 | 0.58 |
| blasted+ pick. + pass. | | D-5* | 3.91/1.07 | 2.61/0.01 | | 0.36 | 0.39 |
| glass | | G-2 | 6.67/1.68 | 3.94/0.08 | | 0.75 | 0.58 |
| blasted+ autoclaved | | H-3 | 7.26/1.59 | 5.13/0.04 | | 0.59 | 0.57 |
| glass | | G-4 | 7.68/1.73 | 5.49/0.03 | | 0.60 | 0.62 |
| blasted+ annealed | | H-2 | 7.71/1.64 | 5.30/0.10 | | 0.66 | 0.56 |

*outside position

** calculated from specific activity

Co-60 = $3.64 \pm 0.70 \mu\text{Ci}/\text{mg}$ Mn-54 = $2.74 \pm 0.44 \mu\text{Ci}/\text{mg}$

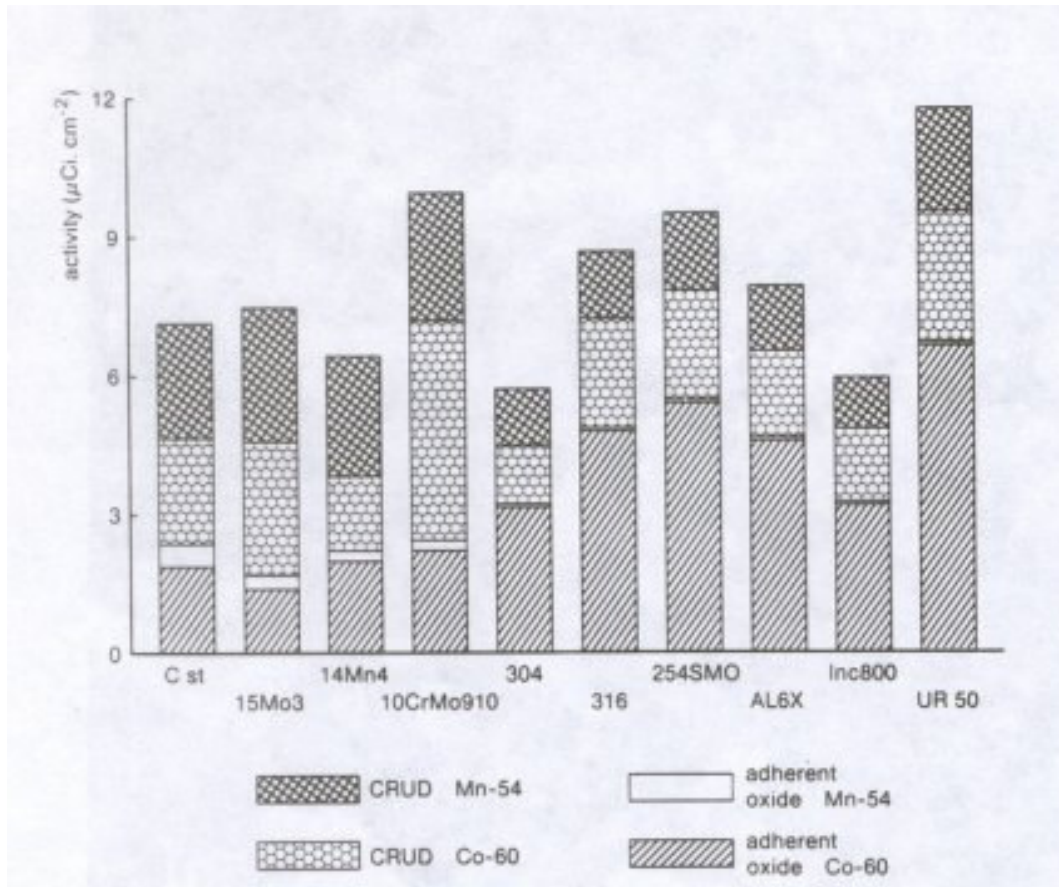


Fig.5. The activities measured on the inside position samples, all glass blasted.

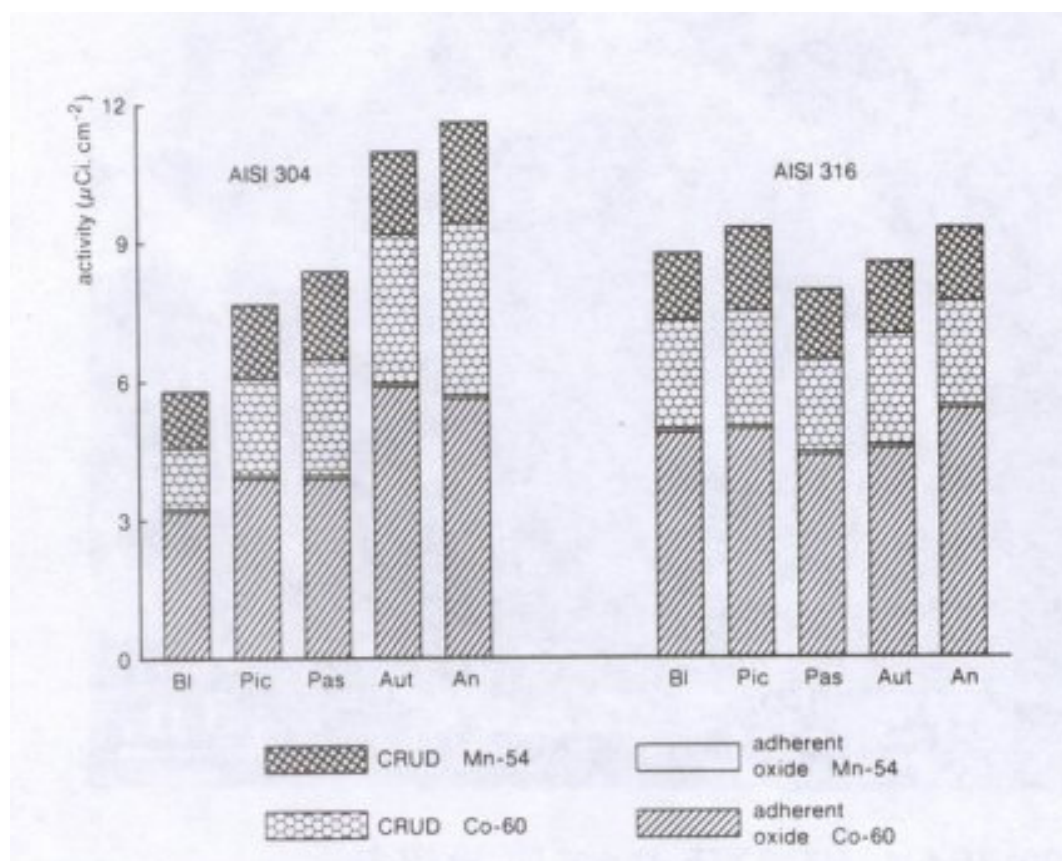


Fig.6. The activities measured on the inside position samples AISI 304 and AISI 316.

Table 6 Activity of the filtered CRUD

| material | position | weight of CRUD (mg - cm ⁻²) | activity Co-60/Mn-54 ($\mu\text{Ci}/\text{cm}^2$) | specific activity Co-60/Mn-54 ($\mu\text{Ci}/\text{mg}$) |
|-----------|----------|--|--|--|
| C-steel | C-5 | 1.9 | 2.29/2.51 | 1.22/1.33 |
| IOCrMo910 | G-5 | 12.5 | 4.78/2.80 | 0.38/0.22 |
| AISI 304 | E-5 | 0.4 | 1.32/1.36 | 3.29/3.40 |
| AISI 316 | D-4 | 0.6 | 2.80/1.56 | 4.67/2.63 |
| 254SM0 | E-4 | 0.7 | 2.42/1.71 | 3.45/2.44 |
| Inc. 800 | F-4 | 0.2 | 1.54/1.12 | 7.68/5.59 |
| Ur50 | B-2 | 0.9 | 2.82/2.26 | 3.13/2.51 |

Seven samples were selected for morphology studies. The CRUD was filtered, dried and weighed (Table 6). The activity of the separated CRUD can be derived from the figures in Tables 4 and 5. The specific Co-60 and Mn-54 activity was determined for the seven filtered samples. The CRUD was mixed with non-active corrosion products because of pitting corrosion of carbon steel and 10CrMo910 and therefore the amount of oxide of these samples was rather high. The specific activities determined for the CRUD on these two samples are therefore not reliable. The value for the Incoloy 800 sample was rather high, which is ascribed to a fault in the weighing procedures.

The following were taken as average values for the specific activity of samples E-5, D-4, E-4 and B-2: $3.64 \pm 0.70 \mu\text{Ci}/\text{mg}$ for Co-60 and $2.74 \pm 0.44 \mu\text{Ci}/\text{mg}$ for Mn-54. The amount of CRUD deposition on the different samples was calculated on the basis of these determined specific activities. These values are also given in Tables 4 and 5.

The duplicates mostly agree but some are quite different. The specimens on the outside of the rack in positions G1, C1, E1, A1 and D5 (marked with one asterisk in the tables) show less CRUD deposition than do the duplicate samples from the inside positions (Fig. 3). The lesser deposition on the outside samples can possibly be explained by a higher flow velocity on these positions.

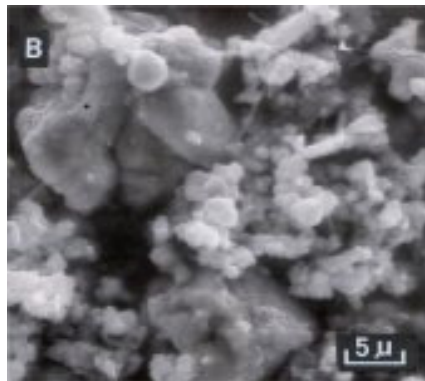
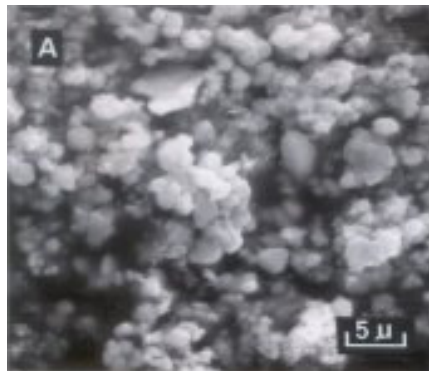
There is a clear difference in the Co-60/Mn-54 ratios of the CRUD and of the adherent oxide. The Co-60 is preferably incorporated in the adherent oxide layer. The ferritic steels show lower activities per unit of surface of the adherent oxide than do the austenitic and ferritic-austenitic steels. There is some indication that the autoclaved and air-annealed samples of AISI 304 have higher activities per unit of surface than the steels subjected to the other surface pre-treatments. This effect was not found for AISI 316.

Morphology

As mentioned before, seven samples were selected for CRUD filtration and morphology studies of CRUD as well as of the adherent oxide. The results have been summarized in Table 7 and some of the scanning electron microscope (SEM) and optical microscope pictures are shown in Figures 7 and 8.

Table 7 Results of SEM studies.

| material | position | CRUD SEM/EDS | | adherent oxide SEM/WDS |
|-----------|----------|-----------------|---------------------|---------------------------|
| C-steel | C-5 | Si | Mn, Fe (Ni) | Fe, O, Si |
| 10CrMo910 | G-5 | Si, Mo [S] | Ti, Cr, Mn, Fe (Ni) | Fe, O, Cr, S, Ni |
| AISI 304 | E-5 | Si, Mo [S] | Cr, Mn, Fe, Ni | |
| AISI316 | D-4 | Si | Mn, Fe, Ni | |
| 254SMO | E-4 | Si | Mn, Fe, Ni | |
| Inc. 800 | F-4 | Si, P | Cr, Mn, Fe, Ni | |
| Ur50 | B-2 | Si, Ca | Mn, Fe, Ni | |



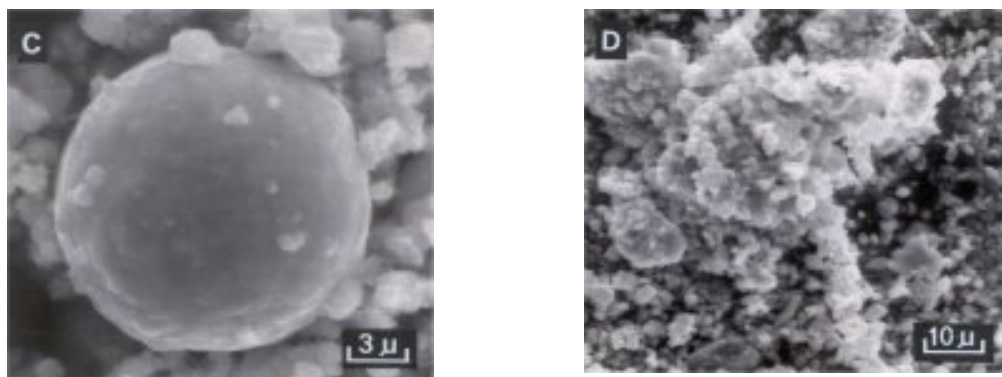


Figure 7. SEM pictures of the CRUD, deposited on C-steel (C5), AISI 304 (E-5), 254SMO (E-4) and Ur50 (B-2)

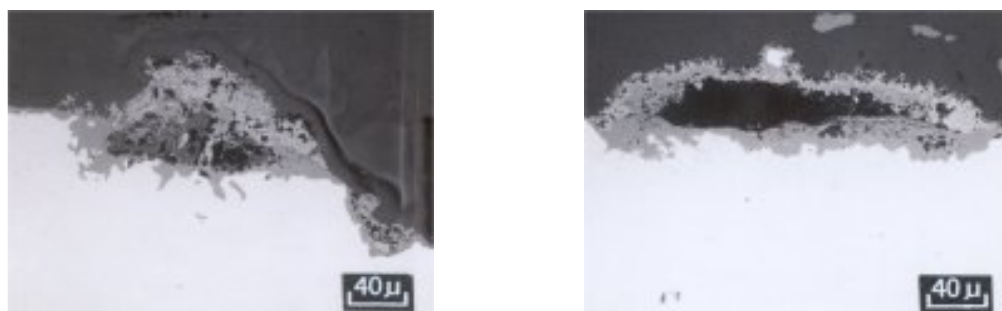


Figure 8. Optical microscopic pictures of the corrosion pits on C-steel (A) and 10CrMo9.10 (B)

The diameter of the CRUD particles ranges from 0.5 to 2.0 micron. The loose oxide removed from the unalloyed and low-alloyed steels contained larger pieces of oxide, i.e. corrosion products of the samples. The texture of the CRUD on the various samples did not differ. Several types of crystals could be distinguished in the CRUD (Fig. 7):

1. small round particles (0.5 to 2 μm)
2. large round spheres (up to 30 μm), covered with small oxide particles
3. needle- or plate-like oxide occasionally.

SEM/EDS studies on the CRUD samples showed the presence of Fe and small amounts of Si, Mn and Ni (0.1 to a few percent by weight). Small amounts of P, Mo or S (the La peak of Mo has the same energy as the Ka peak of S), Ca, Ti and Cr were also found in some of the samples.

Cross-sections of the samples were prepared for microscopic examination. Preliminary visual inspection had shown that C-steel, 15Mo3, 14Mn4 and Fig.7 SEM pictures of the CRUD, deposited on C-steel (C-5), AISI 304 (E-5), 254SMO (E-4) and Ur 50 (B-2) IOCrMo9.10 were pitted. Examples of this pitting corrosion and of the oxide layers formed are shown in Figure 8. The oxide layer on the alloyed steels was rather thin (less than 1 μm).

SEM/WDS studies were performed on carbon steel and IOCrMo9.10. The element mapping of the C-steel sample showed Fe, O and some Si. S, Co and Ni were not present in any significant amount.

Besides Fe, O and Cr, some S and Ni was found in the oxide layer of the IOCrMo9.10 sample. S could originate from inclusions in the steel. Pitting corrosion will start preferably on such inclusions.

Discussion

Results of the examination of corrosion products from, and the CRUD deposition in, 20 nuclear power plants have been published by EPRI (1983). Three possible causes were given for the increase in radiation level:

1. deposition of CRUD
2. incorporation of soluble radioactive corrosion products in the adherent oxide layer (mainly Co-60)
3. isotopic exchange of Co-60 with Co-59.

The EPRI report concluded that the first two causes mentioned were the most important. Low flow velocities will increase the deposition of CRUD. Under strongly oxidizing conditions such as occur in a BWR the chromium in the adherent oxide layer is dissolved as chromate and this leads to the possibility of other soluble corrosion products, e.g. radioactive Co-60, being incorporated.

Other results of interest are that electropolishing of the metal surface and pre-oxidizing in moist air result in a lower exposure rate of AISI 316. Such pretreated piping has been employed at the Monticello Power Plant (EPRI, 1985).

No relationship was found by EPRI between the exposure rate and the quality of the reactor water or the type and capacity of the reactor-water clean-up system and condensate polishing system. There is some indication that small amounts of Zn (originating from corrosion of condenser tubes) in the reactor water inhibit the incorporation of Co-60 in the adherent oxide layer.

The KEMA research shows that the quality of water in the Dodewaard reactor is excellent. However, erosion-corrosion of the carbon steel in the turbine has occurred in the past (Huijbregts, 1984). The corroded carbon steel contained 0.02% of Co. Up to now the reactor has not been decontaminated chemically, so that the remaining Co-59 is activated in the reactor. The Co-60 can be deposited as CRUD and can be incorporated in the adherent oxide of the stainless steel components.

A slight negative effect of the pre-oxidizing treatment of the samples in the Dodewaard reactor was found. These oxide layers thus must have been more Cr-depleted than the naturally formed oxide layers in the reactor. The EPRI pretreatment (annealing in moist air) will result in a different oxide layer and it is probable that this is very critical for the incorporation of Co-60. On the other hand the investigated sample rack had been placed in the reactor vessel and in two-phase flow conditions. These circumstances are probably more oxidizing than those in the RWCU system of the Edwin I Hatch nuclear power plant, in which the electropolished and pre-oxidized (in moist air) EPRI samples had been exposed.

The samples in the Dodewaard rack were mounted in staggered positions. This means that the pressure drop across the rack was high and that the mass flow was lower on the inside samples than it was on the outside samples in the rack. The calculated amounts of CRUD on the outside positions were lower than on samples positioned on the inside. This confirms the assumption of a lower flow in the sample rack. The Co-60 and Mn-54 activity of the adherent oxide layer was plotted versus the total activity (CRUD + adherent oxide) of the samples and versus the calculated amount of deposited CRUD, all calculated per unit of surface (Figures 9 -12). Incorporation of Co-60 in the oxide layers of high-chromium steels depends very much on the amount of deposited CRUD. This effect is less for the C-steel, 15Mo3, 14Mn4, 10CrMo9.10 and Inconel 600 (see Figure 9).

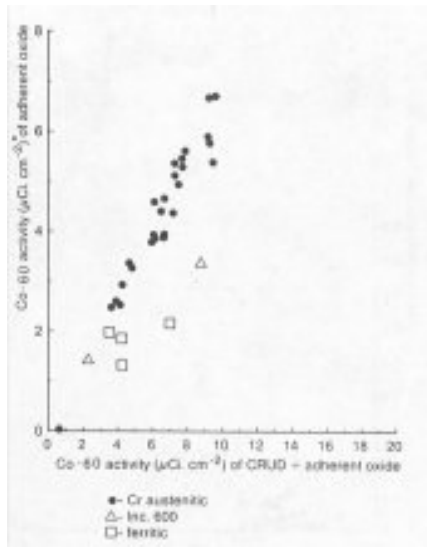


Figure 9. Co-60 activity of the adherent oxide, plotted against the Co-60 activity of the CRUD plus that of the adherent oxide

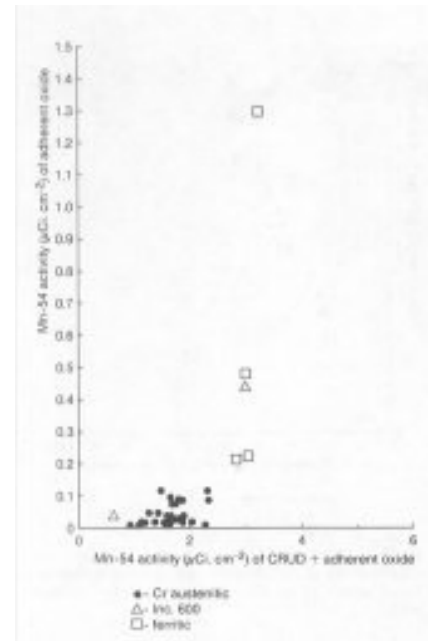


Figure 10. Mn-54 activity of the adherent oxide, plotted against the Mn activity of the CRUD plus that of the adherent oxide.

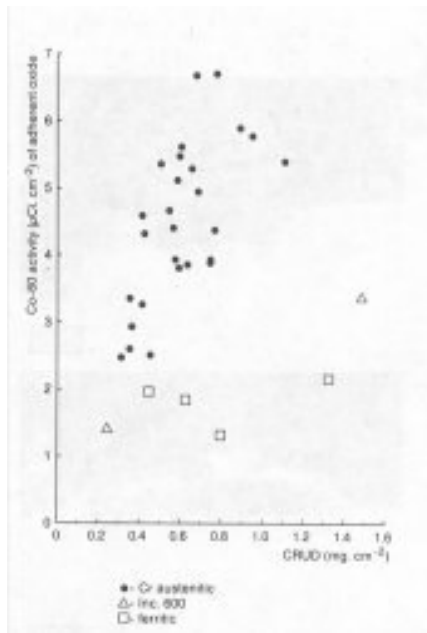


Figure 11. Co-60 activity of the adherent oxide, plotted against the calculated amount of CRUD.

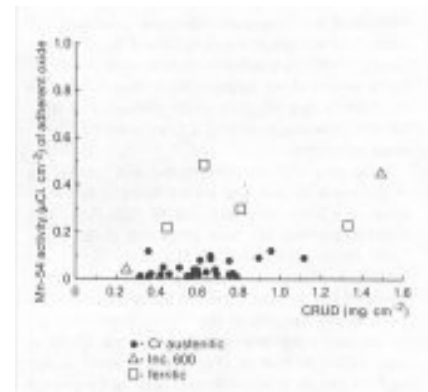


Figure 12. Mn-54 activity of the adherent oxide, plotted against the calculated amount of CRUD.

Concerning the Mn-54 activity, there is some indication that the incorporation in the adherent oxide layer was greater for the ferritic steels than it was for the chromium-containing steels and Inconel 600. It is even possible that the Mn-54 activity of the adherent oxide of the austenitics still originated from some CRUD remaining on the samples.

It is very probable that incorporation of Co-60 takes place via the deposited CRUD. One may assume that the solubility of the Co-60 is higher under the CRUD layer than in the bulk solution. A small potential drop over the CRUD layer could increase the Co solubility, which would be in agreement with the Nernst redox formula. Thicker layers will give higher potential drops and therefore higher Co solubilities as well, resulting in more incorporation. However, the exact mechanism is not yet clear.

Conclusions

Incorporation of Co-60 and Mn-54 in the adherent oxide layers appears to depend very much on the amount of CRUD deposited. This effect of the CRUD layers cannot yet be explained in detail. The local chemical conditions of the water under CRUD presumably change more as the layer becomes thicker.

Incorporation of Co-60 occurs more in the adherent oxide of chromium-containing austenitics than in the unalloyed and low-alloyed steels. Much Mn-54 is incorporated in the adherent oxide layers of both of the latter steel types, which is in contrast to the austenitic steels.

Pre-oxidizing of the austenitic steel AISI 304 gave a higher activity than the pickled and passivated samples. This effect is in contrast with other results and could be explained by differences in test conditions.

References

EPRI (Electric Power Research Institute) 1983 BWR radiation assessment and control program: assessment and control of BWR radiation field. Summary report EPRI (Palo Alto) report NP 3114SY, DE83-902249.

EPRI (Electric Power Research Institute) 1985 Field test and evaluation of electropolishing and preoxidation processes for type 316 stainless steel nuclear grade pipe EPRI (Palo Alto) report NP3832.

Huijbregts, W.M.M. 1984 Erosion-corrosion of carbon steel in wet steam. Materials Performance 23: 97-103.